Competing insulating phases in a dimerized extended Bose-Hubbard model

Aoi Hayashi [1,*] Suman Mondal [2,†] Tapan Mishra [2,3,4,‡] and B. P. Das[1,4]

[1]*Department of Physics, School of Science, Tokyo Institute of Technology, 2-1-2-1, Ookayama, Meguro-ku, Tokyo 152-8550, Japan*
[2]*Department of Physics, Indian Institute of Technology, Guwahati-781039, India*
[3]*School of Physical Sciences, National Institute of Science Education and Research, HBNI, Jatni 752050, India*
[4]*Centre for Quantum Engineering Research and Education, TCG Centres for Research and Education in Science and Technology, Sector V, Salt Lake, Kolkata 700091, India*

We study the ground-state properties of the extended Bose-Hubbard model in a one-dimensional dimerized optical lattice. In the limit of strong on-site repulsion, i.e., hardcore bosons, and strong nearest-neighbor interaction, a stable density-wave (DW) phase is obtained at half-filling as a function of lattice dimerization. Interestingly, at quarter-filling we obtain the signatures of an insulating phase which has the character of both the bond order (BO) and the DW insulators, which we call a bond-order density-wave (BODW) phase. Moreover, we show that for a fixed hopping dimerization there occurs a BO-DW phase crossover as a function of the nearest-neighbor interaction and the BODW phase is more robust when the hopping dimerization is stronger. We further examine the stability of the BODW phase in the limit of finite on-site interactions.

I. INTRODUCTION

The systems of ultracold atoms in optical lattices have been the most versatile quantum simulators enabling to achieve various novel phenomena of nature. Since the seminal observation of the superfluid (SF) to the Mott insulator (MI) phase transition [1] of neutral bosonic atoms in optical lattices, enormous progress has been made in the past two decades leading to the observation of a multitude of physical phenomena. The precise control over the system parameters achieved by suitable manipulation of lattice pontentials and/or the powerful technique of Feshbach resonance has made these systems capable of accessing limits which are difficult to achieve in conventional solid-state systems [2]. This has led to a rapid surge in exploring physics both theoretically, most specifically in the context of the Bose-Hubbard model and its variants, and experimentally [3–6].

One of the most important variants of the Bose-Hubbard (BH) model is the extended Bose-Hubbard (EBH) model which explains the physics of dipolar bosons, which can arise in polar atoms and molecules, and Rydberg excited atoms in optical lattices [7–9] with only nearest-neighbor (NN) interaction. This simple model has been the topic of immense importance in the past [10] and has attracted a renewed interest recently due to its experimental observation [11] in optical lattices using erbium atoms. It has been well established already that the quantum phase diagram corresponding to the EBH model exhibits the gapped density-wave (DW) phases at commensurate densities characterized by the crystalline order [12–15] and the Haldane insulator which exhibits a finite string order parameter [16–18]. Interestingly, the supersolid phases appear at incommensurate densities which possess both the SF and the DW orders as a result of competing on-site and NN interactions [7,10].

On the other hand, optical superlattices which are formed by superimposing two optical lattices of different wavelengths have been shown to reveal a wealth of physical phenomena recently [19–32]. The modified periodicity of the overall lattice in the process favors interesting ground-state phenomena such as the onset of gapped phases at incommensurate densities associated with the primary lattice [23,24,27,28,32–35], symmetry-protected topological phase transition [36–40], frustrated magnetism [41,42], disorder-induced phase transition [43–47], and recently in the context of quantum computation [48]. One of the many variants of the superlattices is the double-well optical lattice which can be formed by superimposing a secondary lattice with a wavelength twice that of the primary lattice. This particular superlattice, which is also known as the dimerized lattice, ensures that the hopping strengths of the particles alternate between the NN bonds. The physics of the double-well lattice (hereafter called the dimerized lattice) is extremely important in the context of condensed-matter physics [49].

For the case of noninteracting fermions and hardcore bosons, the dimerized lattice manifests the interesting symmetry-protected topological phase transition which has been widely discussed in the framework of the celebrated Su-Schrieffer-Heeger (SSH) model [49]. Depending on the hopping dimerization, the system exhibits a gapped bulk spectrum and polarized zero-energy edge modes characterized by the Zak phase [50,51]. The bulk state exhibits finite oscillation in the bond kinetic energy and the system is known to be
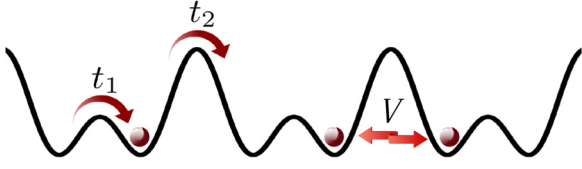
FIG. 1. Double-well lattice structure with dimerized hopping $t_1 > t_2$. V represents the NN interaction between the particles.

in the dimer or BO phase [42,52–55]. Recently, the role of interaction has been investigated in the context the dimerized BH model [35–37,40,56–58] predicting the bulk and edge properties of interacting bosons in optical lattices. A system of three-body constrained (TBC) bosons (allowing a maximum of two bosons per site) on a one-dimensional dimerized lattice was investigated by some of us in Ref. [35]. It was shown that an attractive on-site interaction leads to a BO phase of bound bosonic pairs known as the pair-bond-order (PBO) phase at unit filling which crosses over to an MI phase in the limit of repulsive interaction. However, at half-filling, only a gapped BO phase is stabilized in the repulsive regime. On the other hand, the effect of dimerized NN interaction has been studied extensively for systems of spin-polarized fermions or hardcore bosons [59]. It has been shown that the system goes from the BO phase to a DW phase (phase separation) through an SF phase for repulsive (attractive) NN interaction at half-filling. However, the combined effect of uniform NN interaction, finite on-site interaction, and dimerized hopping at other densities has not been explored in detail.

In this paper we aim to fill the gap by studying the physics of hardcore NN interacting bosons loaded onto a one-dimensional dimerized optical lattice in the framework of the EBH model as depicted in Fig. 1. We analyze the interplay between the hopping dimerization and the NN interactions to explore the emergence of different insulating phases in the ground state of the system. Before going to the details of the results, we briefly highlight the important finding of our analysis. By considering a strong NN interaction, a change in the dimerization results in an insulating phase at quarter-filling which exhibits both the BO and the DW orders. This insulating phase is found to be very sensitive to the change in dimerization strength for fixed NN interactions. Apart from this we obtain the signatures of the BO and DW phases at half-filling and transitions between them. In the end we examine the stability of the nontrivial insulating phase at quarter-filling in the limit of finite on-site interactions.

The remaining part of the paper is organized as follows. In Sec. II we discuss the model which is considered in our studies and the method adopted. We present the results and discussion in Sec. III followed by the conclusions in Sec. IV.

II. MODEL AND APPROACH

The EBH model for dimerized lattice bosons is given by

$$H = - t_1 \sum_{i \in \text{odd}} (a_i^\dagger a_{i+1} + \text{H.c.}) - t_2 \sum_{i \in \text{even}} (a_i^\dagger a_{i+1} + \text{H.c.})$$
$$+ \frac{U}{2} \sum_i n_i(n_i - 1) + V \sum_i n_i n_{i+1}, \quad (1)$$

where a_i and n_i are the bosonic annihilation and number operator, respectively, at sites i; t_1 and t_2 are intra- and intercell hopping strengths; and U and V are the on-site and nearest-neighbor interaction energies. The hopping dimerization is introduced by defining $\delta = t_2/t_1$ and setting $t_1 > t_2$. In the entire simulation we set $t_1 = 1$, which makes all the physical quantities dimensionless.

In our studies, we impose hardcore constraint on bosons by assuming $a_i^{\dagger 2} = 0$, which can be achieved in the limit of $U \to \infty$. The physics of the model shown in Eq. (1) in some limiting situations are well known at half-filling. After a Jordan-Wigner transformation to free fermions, Eq. (1) maps to the interacting SSH model. As highlighted before, in the limit $V = 0$ (the SSH model), the model (1) exhibits a BO phase for any $\delta \neq 1$ at half-filling [35]. On the other hand, it is well known that in the absence of any dimerization (i.e., $\delta = 1$), the model (1) can be suitably mapped to the XXZ model that exhibits a gapless SF to insulating DW phase transition at a critical NN interaction of $V = 2t$ at half-filling. In this work, our aim to explore the emergence of the insulating phases and their nature that may result from the interplay of both δ and V.

To explore the ground-state properties of the many-body Hamiltonian given in Eq. (1) we employ the matrix-product-state-based density matrix renormalization group (DMRG) method [60–63] with a maximum bond dimension of $D = 500$ and an open boundary condition (OBC). We consider system sizes up to $L = 240$ and explore the physics at different densities $\rho = N/L$ of interest, where N is the total number of bosons in the system. We calculate all the physical quantities in the thermodynamic limit ($L = \infty$) using appropriate finite-size extrapolation, unless otherwise mentioned.

III. RESULTS

This section is divided into three parts. To understand the role of interaction, in the first part, we consider a fixed inter-action V and explore the existence of the insulating phases as a function of δ at different densities. In the second part, we explore the effect of V by fixing δ. In the end we study the effect of finite on-site interaction for some exemplary values of δ and V.

A. Fixed interaction

In this subsection, we study the combined effect of both hopping dimerization (i.e., $\delta \neq 1$) and NN interaction (i.e., $V \neq 0$) to explore the possibilities of insulating phases in the system without restricting ourselves to half-filling. For this purpose, we consider a very strong NN interaction, i.e., $V = 10$, and obtain the ground-state phase diagram of the model [Eq. (1)], which is shown in Fig. 2. Interestingly, the phase diagram of Fig. 2 shows three gapped phases corresponding to $\rho = 1/4$, $1/2$, and $3/4$. To properly visualize the phases at $\rho = 1/4$ and $3/4$ we split the phase diagram along the μ axis. The gapped phases are extracted from the behavior of the single-particle excitation gap,

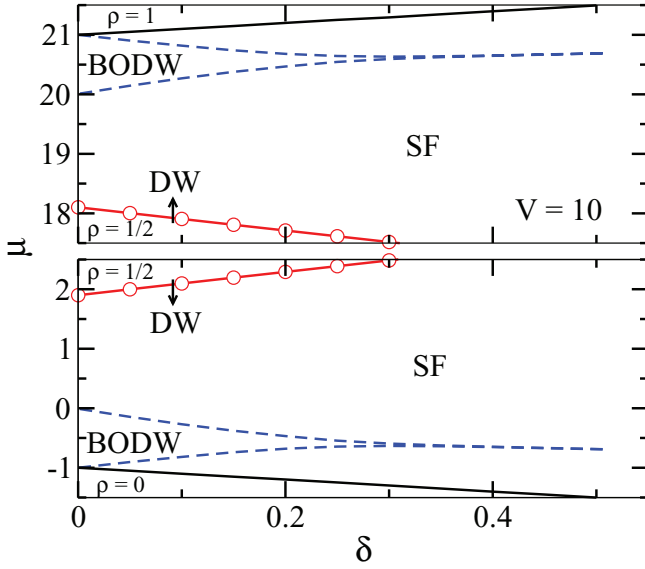$$\Delta_L = \mu_L^+ - \mu_L^-, \quad (2)$$

FIG. 2. The phase diagram depicting the insulating phases in the μ-δ plane ($t_1 = 1$) for the hardcore bosons with $V = 10$. The gapped phases at $\rho = 1/4$ and $3/4$ are the BODW phases bounded by the blue dashed lines, whereas at $\rho = 1/2$, the phase is the DW phase, bounded by red lines with circles. The empty ($\rho = 0$) and full ($\rho = 1$) states are separated by the black solid lines.

where $\mu_L^+ = E_L(N + 1) - E_L(N)$ and $\mu_L^- = E_L(N) - E_L(N - 1)$ are the chemical potentials. Here, $E(N)$ denotes the ground-state energy of the system with N particles. It can be seen from Fig. 2 that the gap remains finite at $\rho = 1/2$ for all values of δ considered (region bounded by the red circles), which is a consequence of large V compared to t_1 and t_2. However, for $\rho = 1/4$ and $3/4$ there is a phase transition to a gapless region as indicated by the smooth closing of the gap Δ_L as a function of δ (region bounded by the blue dashed curves). The solid black lines at the bottom and top in the phase diagram of Fig. 2 correspond to the empty and full states. The gapped and gapless phases can be confirmed by computing the single-particle correlation function, which is given by

$$\Gamma_{ij} = \langle a_i^\dagger a_j \rangle. \tag{3}$$

In Fig. 3 we plot Γ_{ij} against the distance $|i - j|$ in the log-log scale for $\delta = 0.1$ and $\delta = 0.9$, which are within the gapped and gapless regions, respectively, at $\rho = 1/4$ in the phase diagram of Fig. 2. The exponential (power-law) decay of Γ_{ij} for $\delta = 0.1$ (0.9) indicates the gapped (gapless) phase. Note that we calculate Γ_{ij} around the central site of the lattice by considering $i = L/4$ and varying j from $j = L/4 + 1$ to $3L/4$ in order to avoid the edge effects of the finite system with an OBC.

Although Γ_{ij} provides insights about the nature of the phases, it is hard to obtain the phase transition critical points in a situation where the gap or the correlation function varies rather smoothly. This kind of signature at $\rho = 1/4$ and $3/4$ in this case is typical for one-dimensional systems which indicate a Berezinskii-Kosterlitz-Thouless (BKT) type transition [64]. We perform finite-size scaling of the gap Δ_L to accurately quantify the critical δ of transition following Ref. [52].
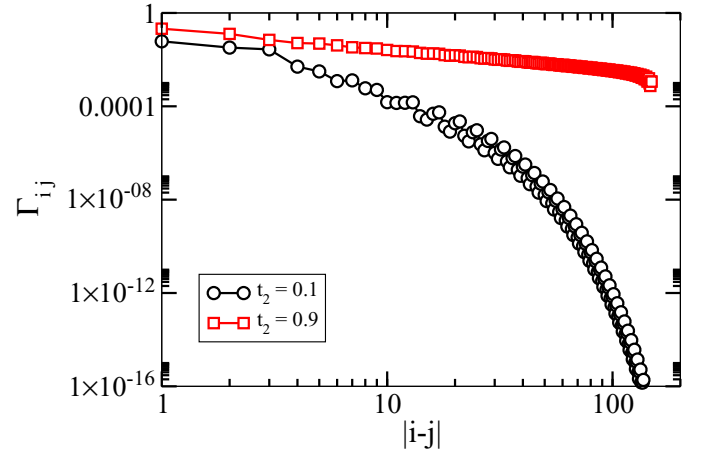

FIG. 3. The correlation function Γ_{ij} is plotted with distance $|i - j|$ in log-log scale for strong dimerization ($\delta = 0.1$) and weak dimerization ($\delta = 0.9$) at $\rho = 1/4$ of a finite system of size $L = 240$. The exponential decay of the curve ($\delta = 0.1$) signifies the gapped phase and a power-law decay ($\delta = 0.9$) indicates a gapless phase.

According to the scaling theory, the quantity

$$L\Delta_L^* = L\Delta_L \left(1 + \frac{1}{2\ln L + C} \right) \tag{4}$$

must be length invariant at a critical value of δ and at the same time exhibit a perfect data collapse as a function of $x_L = \ln L - \frac{a}{\sqrt{|\delta - \delta_c|}}$ near the critical point (δ_c) for suitable values of C and a. As shown in Fig. 4, for $\rho = 1/4$, the perfect crossing of all the curves [Fig. 4(a)] at $\delta \sim 0.506$ and collapse of all the data for different L near the critical point [Fig. 4(b)] indicate a BKT-type phase transition to the gapped phase at a critical point of $\delta_c \sim 0.506$.
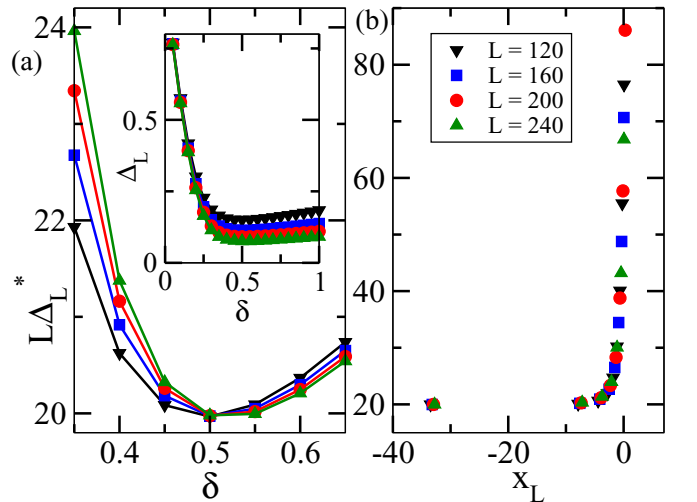

FIG. 4. The finite-size scaling of Δ_L is shown to find the BKT transition point. (a) A perfect crossing of all the curves for different L at $\delta \sim 0.506$ represents the critical point. (b) The collapse of all the data for different L near the critical point ($x_L = \infty$) confirms the BKT transition with $\delta_c \sim 0.506$. Here we display the data points within the gapped phase only. The inset of panel (a) shows Δ_L as a function of δ for different L indicating the gap minimum at $\delta \sim 0.5$.
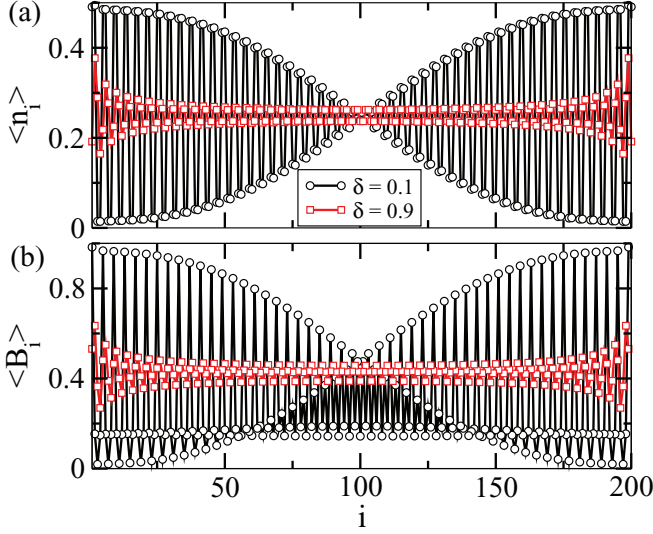
FIG. 5. The values of $\langle n_i \rangle$ and $\langle B_i \rangle$ are plotted in panels (a) and (b), respectively, as a function of the site index i at $\rho = 1/4$ for a system of length $L = 200$ and $V = 10$. The finite oscillations in both $\langle n_i \rangle$ and $\langle B_i \rangle$ for $\delta = 0.1$ (black circles) represent the simultaneous existence of both DW and BO orders, respectively. The oscillations die out for $\delta = 0.9$ (red squares), which indicates the vanishing of the DW and BO orders.

After separating the insulating phases at different densities, we now focus on how to identify the nature of these phases. We find that the gapped phase at $\rho = 1/2$ is a DW phase characterized by a finite oscillation in the real-space density $\langle n_i \rangle$. The DW nature can be well understood by using the density structure factor which is given by

$$S(k) = \frac{1}{L^2} \sum_{i,j} e^{ikr} (\langle n_i n_j \rangle - \langle n_i \rangle \langle n_j \rangle), \qquad (5)$$

where $r = |i - j|$ and k is the crystal momentum. In our simulation we find finite peaks at $k = \pm\pi$ in the structure factor for all values of δ considered, indicating a DW phase where the wave function is a product state with one particle in every other site, i.e.,

$$|\psi\rangle_{DW} = |\dots 1 0 1 0 1 0 1 \dots\rangle. \qquad (6)$$

However, we notice that the insulating phases at $\rho = 1/4$ and $3/4$ are of different natures. Interestingly, they exhibit both BO and DW orders in their character. To characterize this we calculate the expectation values of n_i and the bond energy $B_i = a_i^\dagger a_{i+1} + \text{H.c.}$, which are plotted in Figs. 5(a) and 5(b), respectively, for $\delta = 0.1$ and 0.9. The strong oscillations for $\delta = 0.1$ in both $\langle n_i \rangle$ and $\langle B_i \rangle$ indicate the signatures of both BO and DW orders, respectively. The envelop structure in the density distribution [Fig. 5(a)] is a macroscopic edge effect which appears in a DW ground state due to the presence of the domain wall at the center of the system with a commensurate number of unit cells and an OBC [14,65]. For the same reason the oscillation in B_i also gets modulated [Fig. 5(b)]. In contrast, the oscillations tend to die out for $\delta = 0.9$, although they remain finite due to the finite-size effect. The signatures of DW and BO orders can be well understood from the finite
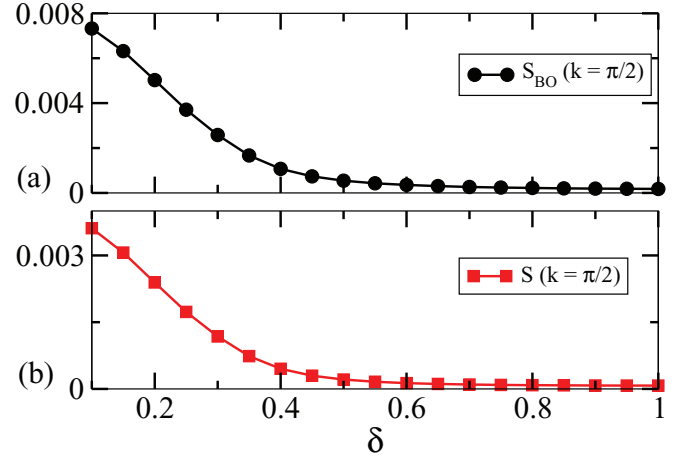

FIG. 6. The extrapolated values of $S_{BO}(k = \pi/2)$ and $S(k = \pi/2)$ are plotted in panels (a) and (b), respectively, with δ at $\rho = 1/4$.

peak in the density structure factor $S(k)$ [Eq. (5)] as well as the BO structure factor $S_{BO}(k)$, which is defined as

$$S_{BO}(k) = \frac{1}{L^2} \sum_{i,j} e^{ikr} \langle B_i B_j \rangle \qquad (7)$$

at finite values of k. For $\rho = 1/4$, we obtain a sharp peak at $k = \pi/2$ for all values of δ within the gapped region of Fig. 2. This behavior suggests that within the gapped region at $\rho = 1/4$, the particles are located at every alternate double well in the lattice, which helps to minimize the energy due to strong repulsive V, and within each occupied double well there is a finite bond energy B_i. We call this insulating phase the bond-order density-wave phase or the BODW phase. As the value of δ becomes larger or the dimerization becomes weaker, the bosons can no more be trapped in the double well. In this limit the bosons can freely move throughout the lattice owing to their incommensurate density turning the system into a gapless SF phase. The BODW to SF phase transition can further be quantified by looking at the behavior of the BO and DW structure factors for different values of δ. In Figs. 6(a) and 6(b) we plot the finite-size extrapolated values of peak heights of $S_{BO}(k = \pi/2)$ and $S(k = \pi/2)$ as a function of δ. The extrapolation is done by using systems of different sizes where the maximum system size is $L = 240$. The vanishing of both $S_{BO}(k = \pi/2)$ and $S(k = \pi/2)$ roughly at $\delta \sim 0.5$ indicates a BODW-SF transition that matches well with the critical point obtained using the gap scaling (see Fig. 4). Note that similar to the $\rho = 1/4$ case, the gapped phase at $\rho = 3/4$ is also found to be a BODW phase.

B. Fixed dimerization

After obtaining the behavior of the system by varying δ for a fixed large V, we explore the physics for a fixed δ and varying V. In this regard, we consider a case of strong dimerization such as $\delta = 0.1$, where the half-filled and quarter-filled sectors belong to the gapped phases (see Fig. 2) and vary V. As already discussed above, in the absence of V and $\delta = 0.1$, there exists only an insulating BO phase at half-filling. On the other hand, for large V, at quarter-filling (half-filling), the
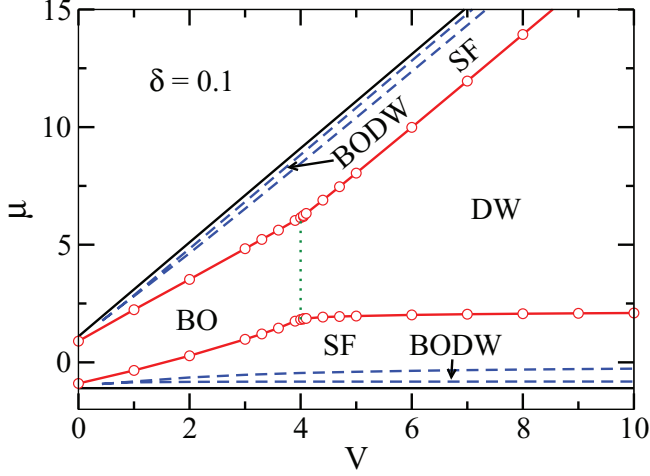
FIG. 7. The phase diagram showing the insulating phases for the hardcore bosons in the μ-V plane ($t_1 = 1$) for $\delta = 0.1$. The insulating phases at $\rho = 1/4$ and $3/4$ are the BODW phases (bounded by the dashed blue lines). At $\rho = 1/2$, the BO-DW transition is marked by the dotted line.

system is in the BODW (DW) phase. Our analysis reveals how these two limits interpolate as a function of V, resulting in a phase diagram as shown in Fig. 7 in the V-μ plane. As the value of V increases, two BODW phases start to appear (opening of the gap) at $\rho = 1/4$ and $3/4$ and the lobes become bigger as a function of V. The phase transitions from the SF to the BODW phase at $\rho = 1/4$ and $3/4$ are found to be of the BKT type. The critical points are calculated from the finite-size scaling of Δ_L following the method discussed before. As the gap variation here is with respect to V, we replace x_L by w_L as

$$w_L = \ln L - \frac{a}{\sqrt{|V - V_c|}}. \tag{8}$$

In Fig. 8 we portray the gap scaling for $\rho = 1/4$ and $\delta = 0.1$. A crossing of all the curves at $V \sim 0.42$ in Fig. 8(a) and a complete collapse of data for different L in Fig. 8(b) yield the BKT transition point at $V_c \sim 0.42$. Similar analysis for $\rho = 3/4$ with $\delta = 0.1$ shows the critical transition point at $V_c \sim 0.43$ as indicated in the phase diagram of Fig. 7. On the other hand, the BO phase at $\rho = 1/2$ becomes a DW phase with increasing V as the NN interaction dominates over the dimerization strength. As both the BO and DW phases are insulating phases, the BO-DW transition can be inferred from a kink in the gap Δ as a function of V. This feature is reflected as the kinks in the μ^+ and μ^- curves (red circles in Fig. 7) at $V \sim 4$. The BO-DW transition point can be quantified by analyzing the corresponding structure factors $S(k)$ and $S_{BO}(k)$. In Figs. 9(a) and 9(b) we plot the extrapolated values of $S(\pi)$ and $S_{BO}(\pi)$ as a function of V for $\delta = 0.1$. The vanishing $S(\pi)$ (solid circles) and finite $S_{BO}(\pi)$ (solid squares) in the regime of small V in Figs. 9(a) and 9(b), respectively, clearly indicate the signature of the BO phase. However, after a critical V_c, the $S(\pi)$ becomes finite, which corresponds to the transition to the DW phase. In order to obtain the critical point for this BO-DW transition we use the derivative of $S(\pi)$ with respect to V. The plot of $dS(\pi)/dV$ as a function of V exhibits a sharp
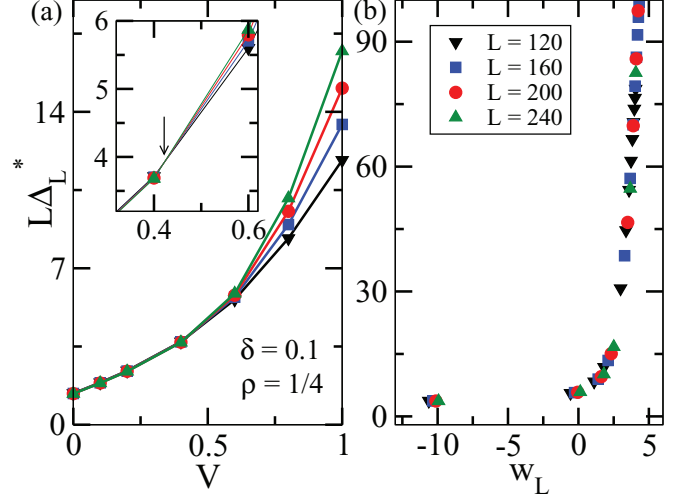

FIG. 8. The finite-size scaling of Δ_L is shown to find the BKT transition point. (a) A perfect crossing of all the curves for different L at $V \sim 0.42$ represents the critical point. The inset shows the magnified plot near the critical point. (b) The collapse of all the data for different L near the critical point ($w_L = \infty$) confirms the BKT transition with $V_c \sim 0.42$. Here we display the data points within the gapped phase only.

peak at $V \sim 4$ as shown in Fig. 9(a) as empty circles. A similar feature in the derivative of $S_{BO}(\pi)$ (empty squares) in Fig. 9(b) confirms the BO-DW transition which is indicated as a dotted line in Fig. 7.

From the above analysis it is evident that the BODW phases exhibit smaller gaps compared to those of the DW and BO phases. We find that the BODW lobe is extremely sensitive to dimerization δ. By considering a slightly weaker dimerization, i.e., $\delta = 0.2$, we obtain the phase diagram as shown in Fig. 10. It can be seen that the gaps at $\rho = 1/4$
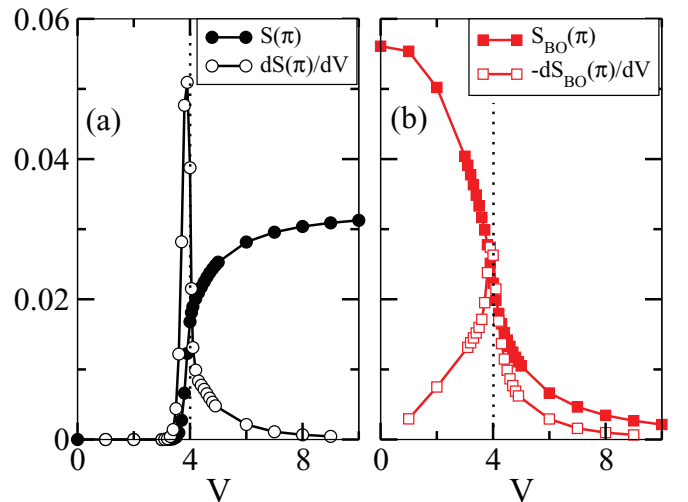

FIG. 9. (a) $S(\pi)$ with its derivative and (b) $S_{BO}(\pi)$ with its derivative are plotted with respect to V for $\delta = 0.1$ and $\rho = 1/2$ corresponding to Fig. 7. The vertical dotted lines at $V \sim 4.0$ correspond to the dotted line shown in Fig. 7 which matches fairly well with the peaks of the derivative functions.
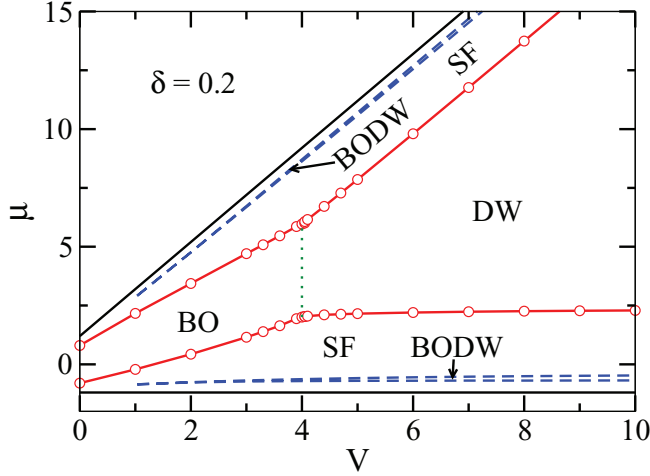
FIG. 10. The phase diagram showing the insulating phases of the hardcore bosons in the μ-V plane ($t_1 = 1$) for $\delta = 0.2$. At $\rho = 1/4$ and $3/4$ the insulating phases are the BODW phases (the region bounded by the dashed blue lines). At $\rho = 1/2$, there exists a BO-DW phase transition marked by the dotted line.

FIG. 11. (a) The variation of ρ with increasing μ is plotted for different combinations of U and V using a finite system of size $L = 80$ and $\delta = 0.1$. The plateaus at $\rho = 1/4$ appear when $V = 10$, indicating the gapped BODW phase. (b) The plots of $S(\pi/2)$ and $S_{BO}(\pi/2)$ as a function of ρ for ($U = 0$, $V = 10$) and ($U = 10$, $V = 10$) confirm the stability of the BODW phase. The inset of panel (a) shows the zoomed in ρ-μ plot of the main figure for $U = 0$ and $V = 0$ for clarity. The inset of panel (b) shows the particle number distribution along the lattice for $\rho = 1/4$ with $V = 10$ and $U = 0$.

and $3/4$ are reduced, thereby shrinking the BODW lobes. However, the effects on the BO and DW phases at $\rho = 1/2$ are very small.

C. Finite on-site interaction

Finally, in this section, we examine the stability of the BODW phase by relaxing the hardcore constraint. For this we allow the finite on-site interaction U of bosons in Eq. (1).

Here, we only discuss the fate of the BODW phase at $\rho = 1/4$. To this end we fix $\delta = 0.1$ and calculate the ρ-μ curves for different combinations of U and V as shown in Fig. 11(a). The finite plateaus at $\rho = 1/4$ for $V = 10$ in the limit of small and large U such as $U = 0$ (red solid curve) and $U = 10$ (green plus) clearly indicate an insulating phase. In order to confirm the nature of this phase, we plot the structure factors $S(\pi/2)$ and $S_{BO}(\pi/2)$ as a function of ρ in Fig. 11(b) for both the combinations, such as ($U = 0$, $V = 10$) and ($U = 10$, $V = 10$). The finite peaks at $\rho = 1/4$ in both the structure factors confirms the stability of the BODW phase. In the inset of Fig. 11(b), we plot $\langle n_i \rangle$ at $\rho = 1/4$ for $V = 10$ and $U = 0$ where each double well has one particle followed by an empty double well, confirming the existence of the BODW phase. The stability of the BODW phase in the vanishing U limit can be described from the perspective of energy cost due to interactions. If we start from the BODW phase at $U = \infty$ and decrease U below the hardcore limit, the particles are still restricted to hop to the other double wells that are either empty or filled with a dimer which costs an increase in energy due to V. On the other hand, the ρ-μ curves for $V = 0$ do not show any plateaus, which indicates that the system is in the gapless SF phases [see Fig. 11(a)]. The inference that can be drawn from the above analysis is that this BODW phase appears due to the interplay between the long-range interaction and hopping dimerization alone, and the role of U is not significant.
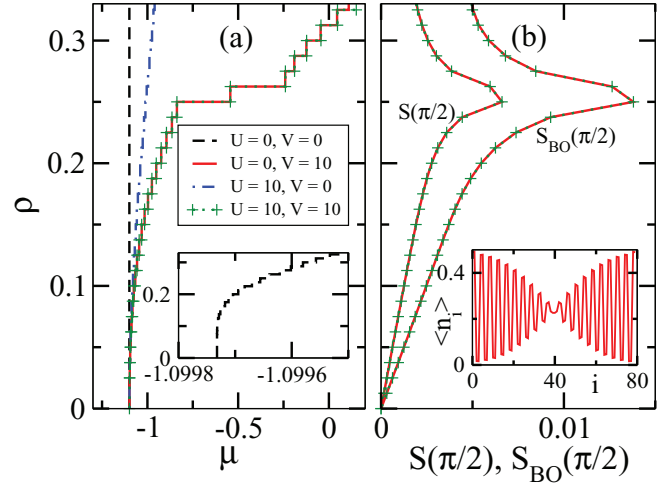
IV. CONCLUSIONS

In conclusion, we have studied the physics of the ground state of a system of interacting hardcore bosons in a one-dimensional optical lattice with hopping dimerization. By using the DMRG method, we have predicted the emergence of various insulating phases and associated phase transitions. We have shown that in the presence of large NN interaction, the system exhibits a DW phase which remains stable for all values of dimerization strengths. Interestingly, at quarter-fillings, we have obtained the signatures of an insulating phase that exhibits both the bond order and the density wave orders which we call the BODW phase. Moreover, we have obtained a SF-BODW phase transition as a function of the dimerization strength which is of the BKT universality class. On the other hand, by fixing the dimerization strength, there occurs a BO-DW phase transition at half-filling as a function of the NN interaction. In this case also, we have obtained a SF-BODW phase transition at quarter-filling. It is found that the BODW phase is extremely sensitive to the dimerization strength. In the end we have predicted the stability of the BODW phase in the limit of finite on-site interaction.

Our findings predict various insulating phases including the BODW phase at quarter-filling which is a result of both the hopping dimerization and the NN interaction. These predictions can, in principle, be realized in experiments involving ultracold dipolar atoms in optical lattices. As already mentioned, the lattice model we have considered resembles a double-well optical lattice which has been realized in recent experiments by superimposing an optical lattice with another lattice having a wavelength half that of the first one [51]. Moreover, by arranging the one-dimensional lattice in a zig-zag structure and by aligning the dipoles in a suitable direction

one can restrict the long-range dipole-dipole interaction to the nearest neighbors only [66]. As a possible future direction, it will be interesting to explore the topological properties of the model considered at quarter-filling. As the system exhibits a gap in this limit, it may favor a topological phase transition which can be studied by changing the hopping dimerization in the framework of the interacting SSH model [37].

[1] M. Greiner, O. Mandel, T. Esslinger, T. W. Hänsch, and I. Bloch, Nature (London) **415**, 39 (2002).

[2] I. Bloch, J. Dalibard, and W. Zwerger, Rev. Mod. Phys. **80**, 885 (2008).

[3] F. Schäfer, T. Fukuhara, S. Sugawa, Y. Takasu, and Y. Takahashi, Nat. Rev. Phys. **2**, 411 (2020).

[4] C. Gross and I. Bloch, Science **357**, 995 (2017).

[5] I. Bloch, J. Dalibard, and S. Nascimbène, Nat. Phys. **8**, 267 (2012).

[6] M. Lewenstein, A. Sanpera, and V. Ahufinger, Contemp. Phys. **54**, 112 (2013).

[7] T. Lahaye, C. Menotti, L. Santos, M. Lewenstein, and T. Pfau, Rep. Prog. Phys. **72**, 126401 (2009).

[8] K.-K. Ni, S. Ospelkaus, M. H. G. de Miranda, A. Pe'er, B. Neyenhuis, J. J. Zirbel, S. Kotochigova, P. S. Julienne, D. S. Jin, and J. Ye, Science **322**, 231 (2008).

[9] T. F. Gallagher and P. Pillet, *Advances in Atomic, Molecular, and Optical Physics* (Academic, San Diego, 2008), Vol. 56, pp. 161–218.

[10] M. Baranov, Phys. Rep. **464**, 71 (2008).

[11] S. Baier, M. J. Mark, D. Petter, K. Aikawa, L. Chomaz, Z. Cai, M. Baranov, P. Zoller, and F. Ferlaino, Science **352**, 201 (2016).

[12] T. D. Kühner, S. R. White, and H. Monien, Phys. Rev. B **61**, 12474 (2000).

[13] G. G. Batrouni, R. T. Scalettar, G. T. Zimanyi, and A. P. Kampf, Phys. Rev. Lett. **74**, 2527 (1995).

[14] T. Mishra, R. V. Pai, S. Ramanan, M. S. Luthra, and B. P. Das, Phys. Rev. A **80**, 043614 (2009).

[15] R. Kraus, K. Biedroń, J. Zakrzewski, and G. Morigi, Phys. Rev. B **101**, 174505 (2020).

[16] E. G. Dalla Torre, E. Berg, and E. Altman, Phys. Rev. Lett. **97**, 260401 (2006).

[17] E. Berg, E. G. Dalla Torre, T. Giamarchi, and E. Altman, Phys. Rev. B **77**, 245119 (2008).

[18] D. Rossini and R. Fazio, New J. Phys. **14**, 065012 (2012).

[19] J. Sebby-Strabley, M. Anderlini, P. S. Jessen, and J. V. Porto, Phys. Rev. A **73**, 033605 (2006).

[20] J. Sebby-Strabley, B. L. Brown, M. Anderlini, P. J. Lee, W. D. Phillips, J. V. Porto, and P. R. Johnson, Phys. Rev. Lett. **98**, 200405 (2007).

[21] M. Anderlini, P. J. Lee, B. L. Brown, J. Sebby-Strabley, W. D. Phillips, and J. V. Porto, Nature (London) **448**, 452 (2007).

[22] S. Fölling, S. Trotzky, P. Cheinet, M. Feld, R. Saers, A. Widera, T. Müller, and I. Bloch, Nature (London) **448**, 1029 (2007).

[23] M. Singh, A. Dhar, T. Mishra, R. V. Pai, and B. P. Das, Phys. Rev. A **85**, 051604(R) (2012).

[24] M. Singh and T. Mishra, Phys. Rev. A **94**, 063610 (2016).

[25] A. Dhar, T. Mishra, R. V. Pai, and B. P. Das, Phys. Rev. A **83**, 053621 (2011).

[26] A. Dhar, M. Singh, R. V. Pai, and B. P. Das, Phys. Rev. A **84**, 033631 (2011).

[27] R. Roth and K. Burnett, Phys. Rev. A **68**, 023604 (2003).

[28] F. Schmitt, M. Hild, and R. Roth, Phys. Rev. A **80**, 023621 (2009).

[29] G. Roux, T. Barthel, I. P. McCulloch, C. Kollath, U. Schollwöck, and T. Giamarchi, Phys. Rev. A **78**, 023628 (2008).

[30] S. Peil, J. V. Porto, B. L. Tolra, J. M. Obrecht, B. E. King, M. Subbotin, S. L. Rolston, and W. D. Phillips, Phys. Rev. A **67**, 051603(R) (2003).

[31] P. Cheinet, S. Trotzky, M. Feld, U. Schnorrberger, M. Moreno-Cardoner, S. Fölling, and I. Bloch, Phys. Rev. Lett. **101**, 090404 (2008).

[32] B.-L. Chen, S.-P. Kou, Y. Zhang, and S. Chen, Phys. Rev. A **81**, 053608 (2010).

[33] I. Danshita, J. E. Williams, C. A. R. Sá de Melo, and C. W. Clark, Phys. Rev. A **76**, 043606 (2007).

[34] S. Lahiri, S. Mondal, M. Singh, and T. Mishra, Phys. Rev. A **101**, 063624 (2020).

[35] S. Mondal, S. Greschner, and T. Mishra, Phys. Rev. A **100**, 013627 (2019).

[36] F. Grusdt, M. Höning, and M. Fleischhauer, Phys. Rev. Lett. **110**, 260405 (2013).

[37] S. Greschner, S. Mondal, and T. Mishra, Phys. Rev. A **101**, 053630 (2020).

[38] S. Mondal, S. Greschner, L. Santos, and T. Mishra, Phys. Rev. A **104**, 013315 (2021).

[39] S. Ryu and Y. Hatsugai, Phys. Rev. Lett. **89**, 077002 (2002).

[40] M. Di Liberto, A. Recati, I. Carusotto, and C. Menotti, Phys. Rev. A **94**, 062704 (2016).

[41] M. Aidelsburger, M. Atala, S. Nascimbène, S. Trotzky, Y.-A. Chen, and I. Bloch, Phys. Rev. Lett. **107**, 255301 (2011).

[42] A. Dhar, T. Mishra, R. V. Pai, S. Mukerjee, and B. P. Das, Phys. Rev. A **88**, 053625 (2013).

[43] H. P. Lüschen, S. Scherg, T. Kohlert, M. Schreiber, P. Bordia, X. Li, S. Das Sarma, and I. Bloch, Phys. Rev. Lett. **120**, 160404 (2018).

[44] M. Schreiber, S. S. Hodgman, P. Bordia, H. P. Lüschen, M. H. Fischer, R. Vosk, E. Altman, U. Schneider, and I. Bloch, Science **349**, 842 (2015).

[45] X. Li and S. Das Sarma, Phys. Rev. B **101**, 064203 (2020).

[46] G. Roati, C. D'Errico, L. Fallani, M. Fattori, C. Fort, M. Zaccanti, G. Modugno, M. Modugno, and M. Inguscio, Nature (London) **453**, 895 (2008).

[47] A. Padhan, M. Kanti Giri, S. Mondal, and T. Mishra, Phys. Rev. B **105**, L220201 (2022).

[48] B. Yang, H. Sun, C.-J. Huang, H.-Y. Wang, Y. Deng, H.-N. Dai, Z.-S. Yuan, and J.-W. Pan, Science **369**, 550 (2020).

[49] W. P. Su, J. R. Schrieffer, and A. J. Heeger, Phys. Rev. Lett. **42**, 1698 (1979).

[50] J. Zak, Phys. Rev. Lett. **62**, 2747 (1989).

[51] M. Atala, M. Aidelsburger, J. T. Barreiro, D. Abanin, T. Kitagawa, E. Demler, and I. Bloch, Nat. Phys. **9**, 795 (2013).

[52] T. Mishra, J. Carrasquilla, and M. Rigol, Phys. Rev. B **84**, 115135 (2011).

[53] T. Mishra, R. V. Pai, S. Mukerjee, and A. Paramekanti, Phys. Rev. B **87**, 174504 (2013).

[54] T. Mishra, R. V. Pai, and S. Mukerjee, Phys. Rev. A **89**, 013615 (2014).

[55] T. Mishra, S. Greschner, and L. Santos, Phys. Rev. A **91**, 043614 (2015).

[56] M. Di Liberto, A. Recati, I. Carusotto, and C. Menotti, Eur. Phys. J.: Spec. Top. **226**, 2751 (2017).

[57] Y. Kuno and Y. Hatsugai, Phys. Rev. Research **2**, 042024(R) (2020).

[58] J. Fraxanet, D. González-Cuadra, T. Pfau, M. Lewenstein, T. Langen, and L. Barbiero, Phys. Rev. Lett. **128**, 043402 (2022).

[59] M. Kohmoto, M. den Nijs, and L. P. Kadanoff, Phys. Rev. B **24**, 5229 (1981).

[60] S. R. White, Phys. Rev. Lett. **69**, 2863 (1992).

[61] S. R. White, Phys. Rev. B **48**, 10345 (1993).

[62] U. Schollwöck, Rev. Mod. Phys. **77**, 259 (2005).

[63] U. Schollwöck, Ann. Phys. **326**, 96 (2011), January 2011 Special Issue.

[64] M. A. Cazalilla, R. Citro, T. Giamarchi, E. Orignac, and M. Rigol, Rev. Mod. Phys. **83**, 1405 (2011).

[65] S. Stumper and J. Okamoto, Phys. Rev. A **101**, 063626 (2020).

[66] S. de Léséleuc, V. Lienhard, P. Scholl, D. Barredo, S. Weber, N. Lang, H. P. Büchler, T. Lahaye, and A. Browaeys, Science **365**, 775 (2019).